Supporting Information

Grizenkova et al. 10.1073/pnas.1208917109

SI Methods

Verification of Microarray Data. Microarray data were verified by real-time PCR using a 7500 Fast Real-Time PCR system (Applied Biosystems). In the first instance, the same samples were used as for the microarray experiments ($n = 5$) and subsequently these were repeated in an additional independent panel ($n = 5$ per strain). RNA was extracted and reverse transcribed as previously described (1). For initial testing, the top 30 genes were amplified with Power SYBR Green PCR Master Mix (Applied Biosystems) according to the manufacturer's instructions. All genes were duplexed separately with each of three endogenous controls (*GAPDH*, *Cyclophilin*, and *Glucuronidase β*). Cycling conditions were as follows: 95 °C for 10 mins; 95 °C for 15 s, 60 °C for 60 s for 40 cycles followed by a dissociation step of 95 °C for 15 s; 60 °C for 60 s, 95 °C for 15 s. Genes that replicated the microarray results using SYBR green were further tested using 5′Fam and 3′Tamra dual-labeled probes. All genes were duplexed separately with *GAPDH* and *β-actin* endogenous controls as previously described (2).

***Hspa13* (*Stch*) mRNA Expression in Tg222 and Tc1 Mice.** RNA was extracted from mouse brains and reverse transcribed as previously described (1). First choice human brain reference total RNA (Ambion) comprises a pool of $n = 23$ donors and was used as a control for human-specific *Hspa13*. *Hspa13* expression was determined using real-time PCR with either mouse- or human-specific primers. For mouse *Hspa13* the primers were as follows: forward 5′-GGACAGGAAAAGTGAAGGTGATTC-3′, reverse 5′-CATCACCGTCCGTGAAGGA-3′, probe 5′-Fam-ACGGGCATATCAGCATCCCCAGC-Tamra-3′. For human *HSPA13*, the primers were as follows: forward 5′-GAACCT-CACAGTAGTGACACTGAACTG-3′, reverse 5′-GGCCAC-GTCCAAACCA-3′, probe 5′-Fam-AACTTTCCTCAGCAG-ATGACCATCGCG-Tamra-3′. All samples were run in triplicate. The *Hspa13* probes were duplexed in turn with each of three Vic-labeled endogenous controls (*GAPDH*, *β-actin*, and *Thy-1*) (2). The geometric mean of these data was used for statistical analyses.

Sequencing. Genomic DNA was extracted from postmortem tail samples as previously described (3). The exons and intron boundaries of *STCH* were sequenced in Tc1 mice. Genomic sequence and structure was obtained from the University of California Santa Cruz genome browser (http://genome.ucsc.edu/). For sequencing human *STCH* cDNA, total RNA was extracted from a Tc1 mouse brain and reverse transcribed as previously described (1). Primers for PCR products were designed using Primer 3 (http://frodo.wi.mit.edu/). PCR products were generated and sequenced as previously described (2). Sequencing was carried out on an Applied Biosystems 3730XL capillary sequencer.

Western Blotting. For detection of PrP^{Sc} by Western blotting 10% (wt/vol), brain homogenates in Dulbecco's phosphate-buffered saline were prepared by ribolysing. Samples were benzonase treated and proteinase K digested (50 μg/mL of proteinase K for 1 h at 37 °C) and blotted as described previously (4). PrP was detected with anti-PrP monoclonal antibody ICSM35 (D-Gen) (5) and alkaline–phosphatase-conjugated antimouse IgG secondary antibody (Sigma-Aldrich) developed in the chemiluminescent substrate CDP-Star (Tropix). For nonprion-infected material, samples were prepared as above but without proteinase K digestion. For the detection of Hspa13 and Sod1, proteins were resolved on 10% and 16% Tris-glycine Novex gels (Invitrogen), respectively, and transferred to nitrocellulose membrane (Pall Life Sciences). Human Hspa13 was detected with the rabbit polyclonal antibody 12667–2-AP (0.16 μg/mL) (Protein Tech Group) and Sod1 was detected with the rabbit polyclonal antibody ab16831(0.5 μg/mL) (Abcam). Anti–β-actin mouse monoclonal antibody clone AC-15 (0.05 μg/mL) (Sigma) was also included on these blots as a loading control. Secondary antibodies used were IRDye800CW conjugated goat antirabbit IgG (Li-Cor) and IRDye680 conjugated goat antimouse IgG (Li-Cor) both used at a final concentration of 0.1 μg/mL. Fluorescence was detected using an Odyssey infrared imager (Li-Cor).

Quantification of PrP^c by Enzyme-Linked Immunosorbent Assay (ELISA). Ten percent (wt/vol) brain homogenates were used to measure endogenous levels of PrP^c by ELISA (6). PrP^c was captured by anti-PrP monoclonal antibody ICSM18 (D-Gen) and detected using biotinylated anti-PrP monoclonal antibody ICSM35 (D-Gen) and streptavidin-horseradish peroxidize conjugate (Dako). A Pierce bicinchoninic acid (BCA) protein assay kit (Thermo Scientific) was used to measure the total protein concentration according to the manufacturer's instructions.

1. Lloyd SE, et al. (2009) HECTD2 is associated with susceptibility to mouse and human prion disease. *PLoS Genet* 5:e1000383.
2. Lloyd SE, Maytham EG, Grizenkova J, Hummerich H, Collinge J (2010) A Copine family member, Cpne8, is a candidate quantitative trait gene for prion disease incubation time in mouse. *Neurogenetics* 11:185–191.
3. Lloyd SE, et al. (2001) Identification of multiple quantitative trait loci linked to prion disease incubation period in mice. *Proc Natl Acad Sci USA* 98:6279–6283.
4. Wadsworth JD, et al. (2001) Tissue distribution of protease resistant prion protein in variant CJD using a highly sensitive immuno-blotting assay. *Lancet* 358:171–180.
5. Asante EA, et al. (2002) BSE prions propagate as either variant CJD-like or sporadic CJD-like prion strains in transgenic mice expressing human prion protein. *EMBO J* 21: 6358–6366.
6. Wadsworth JD, et al. (2006) Phenotypic heterogeneity in inherited prion disease (P102L) is associated with differential propagation of protease-resistant wild-type and mutant prion protein. *Brain* 129:1557–1569.

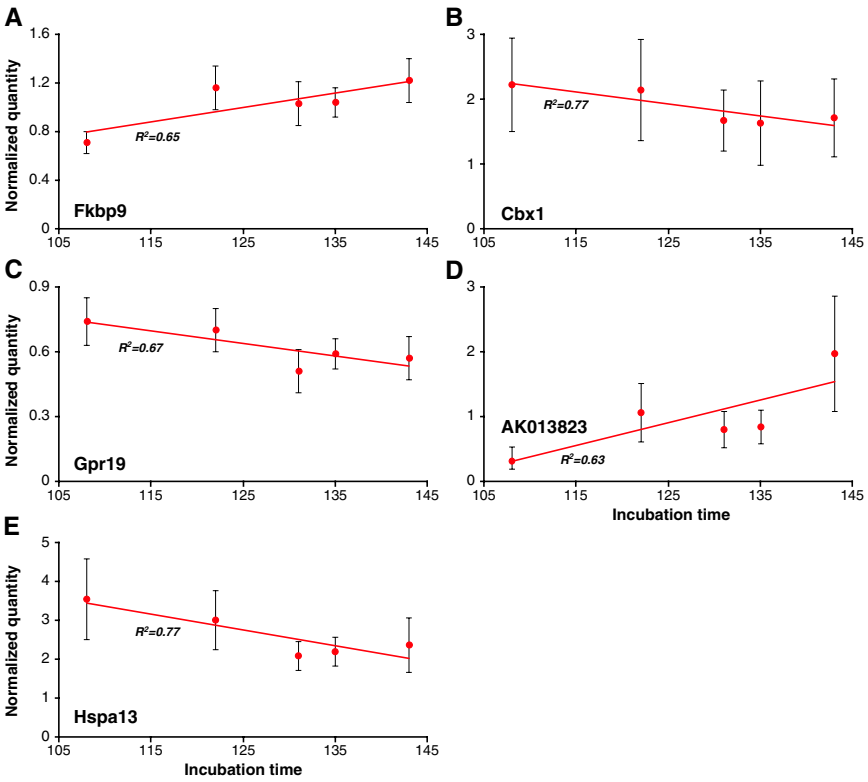

Fig. S1. Real-time RT-PCR verification of microarray data showing correlation of gene expression level with incubation time. Mean incubation time of each of five inbred mouse strains inoculated with the Chandler/Rocky Mountain Laboratory (RML) prion strain is measured in days and is shown on the *x* axis (NZW/OlaHsd, SJL/OlaHsd, FVB/NHsd, SWR/OlaHsd, and C57BL/6JOlaHsd). Data are shown for $n = 10$ animals from each strain (except *Gpr19* where $n = 5$). The GAPDH normalized quantity for each transcript is represented on the *y* axis (mean ± SD). R^2 represents the square of the Pearson product moment correlation coefficient. (*A*) *Fkbp9*, (*B*) *Cbx1*, (C) *Gpr195*, (*D*) *AK013823*, and (*E*) *Hspa13* (*Stch*).

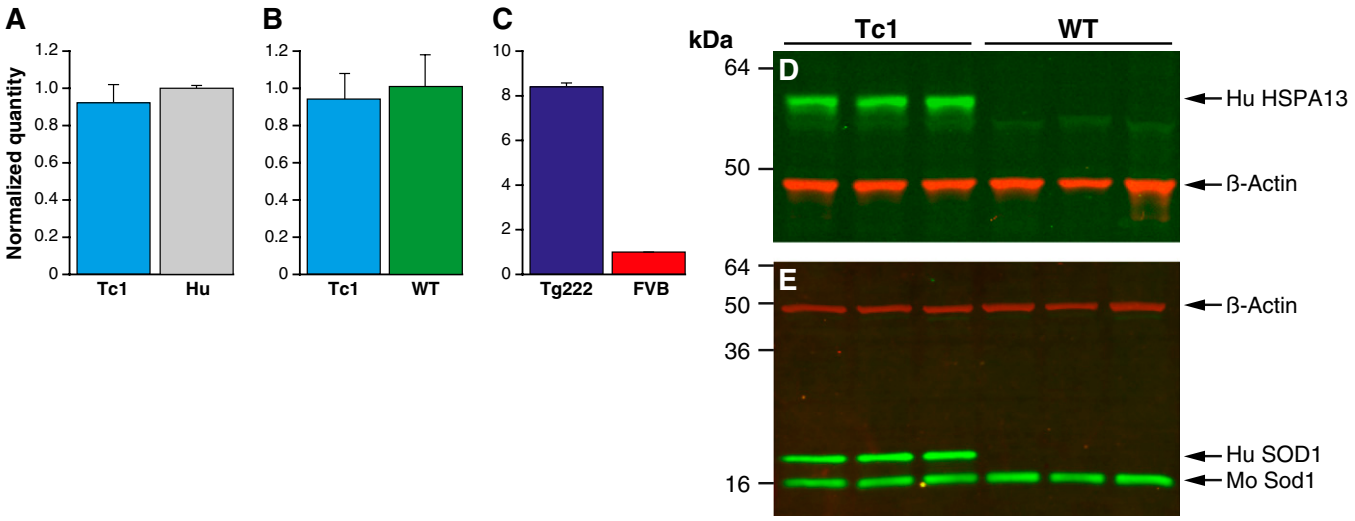

Fig. S2. Hspa13 and Sod1 expression. *A–C* show quantification of *Hspa13* mRNA expression in whole brain by real-time RT-PCR. All samples were run in triplicate. All mouse samples were duplexed for *Hspa13* (Fam labeled) (mouse or human specific) and each of three endogenous controls *GAPDH*, *β-actin*, or *Thy-1* (Vic-label). For human control samples, only *GAPDH* and *β-actin* were used. Expression level is expressed in arbitrary units and normalized by the geometric mean of the quantity of the endogenous controls (*y* axis) and expressed relative to the control. Error bars represent the SD. (*A*) Human-specific HSPA13 probe for Tc1 ($n = 7$) and human brain (Hu) (first choice human brain reference total RNA pool of $n = 23$; Ambion). (*B*) Mouse-specific Hspa13 probe for Tc1 ($n = 6$) and wild-type litter mate controls ($n = 4$). No significant difference was seen between Tc1 and controls for either human- or mouse-specific *Hspa13*. (*C*) Comparison of mouse *Hspa13* expression in Tg222 ($n = 3$) and FVB controls ($n = 3$). Tg222 shows an approximately eightfold increase in *Hspa13* mRNA expression relative to FVB controls ($P < 0.0001$, *t* test). *D* and *E* show expression of HSA13 and SOD1 proteins in Tc1 mice. Western blots of 10% (wt/vol) brain homogenates from Tc1 ($n = 3$) and wild-type litter mate controls ($n = 3$). (*A*) Immunoblotted with rabbit polyclonal antihuman HSPA13 antibody (Protein Tech Group) and detected with IRDye800CW (green) conjugated-goat antirabbit IgG (Li-Cor). Human HSPA13 is seen only in Tc1 mice running at ~60 kDa. Mouse Hspa13 is not well detected with this antibody. (*B*) Immunoblotted with rabbit polyclonal antihuman SOD1(Abcam) and detected with IRDye800CW (green) conjugated-goat antirabbit IgG (Li-Cor). Human SOD1 is detected only in Tc1 mice and mouse sod1 is seen in both Tc1 and controls (16–18 kDa). Anti–β-actin mouse monoclonal antibody (Sigma) was also included on both blots as a loading control and was detected using IRDye680 (red) conjugated-goat antimouse IgG (Li-Cor). Fluorescence was visualized using an Odyssey infrared imager (Li-Cor).

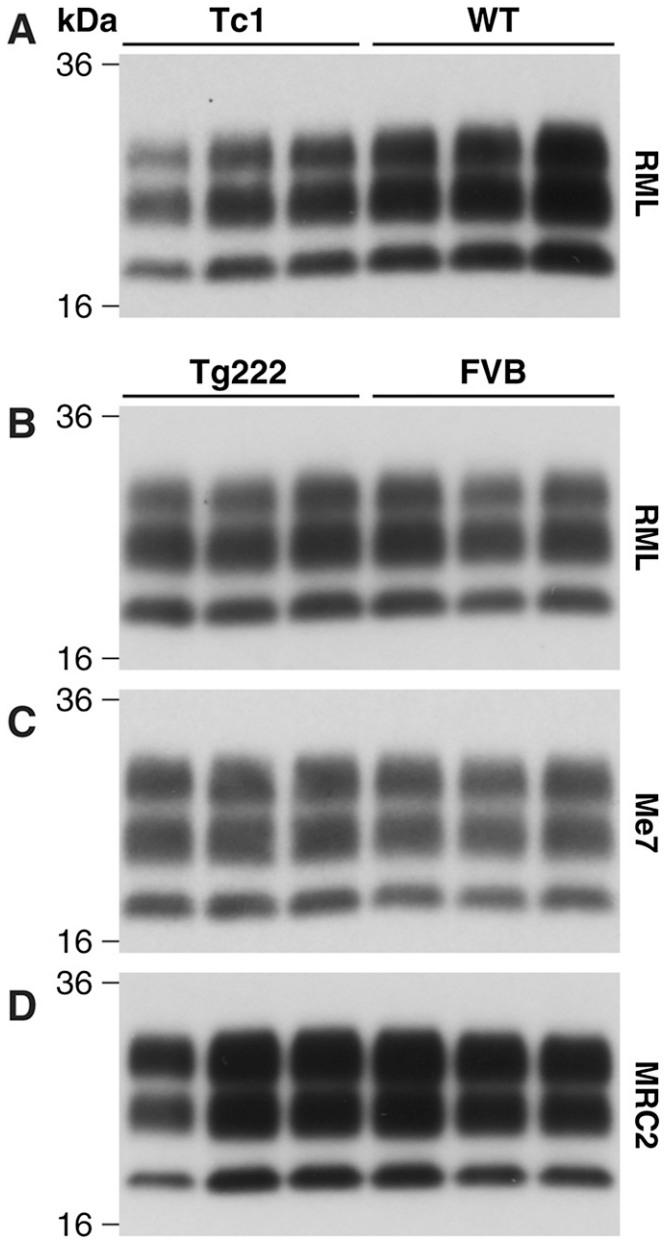

Fig. S3. Western blots of PrP^{Sc} from mouse brains following prion transmission. Ten percent (wt/vol) brain homogenates (n = 3 per group) were digested with proteinase K and immunoblotted with anti-PrP monoclonal antibody ICSM35 (D-Gen). (*A*) Transmission of Chandler/RML prions to Tc1 and wild-type litter mate controls. No differences were seen between the two groups. (*B–D*) Transmission of three different prion strains to Tg222 (Hspa13 overexpressors) and FVB/NHsd wild-type controls. (*B*) Chandler/RML, mouse-adapted scrapie. (*C*) ME7, mouse-adapted scrapie. (*D*) MRC2, mouse-adapted bovine spongiform encephalopathy (BSE). No differences were seen between the two groups regardless of prion strain.

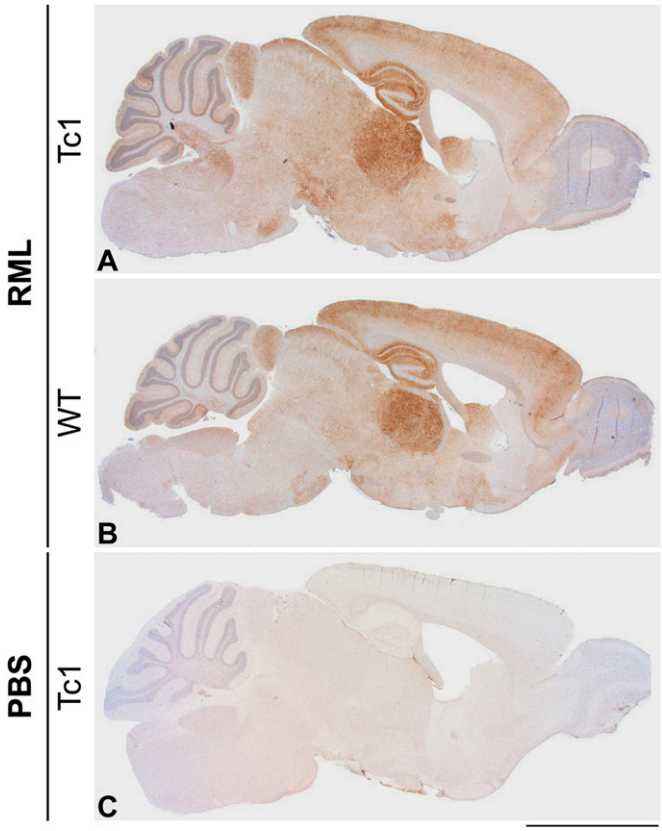

Fig. S4. PrP^{Sc} distribution in whole brain sections for Chandler/RML transmission to Tc1 mice. (*A*) Tc1, (*B*) wild-type litter mate control, and (*C*) PBS control inoculated Tc1. Prion deposition was visualized with anti-PrP monoclonal antibody ICSM35 (D-Gen). Overall, the pattern of PrP^{Sc} distribution is characteristic of the prion strain and shows no difference between Tc1 and wild-type groups. No signal is detected for PBS control inoculated Tc1. (Scale bar, 3 mm.)

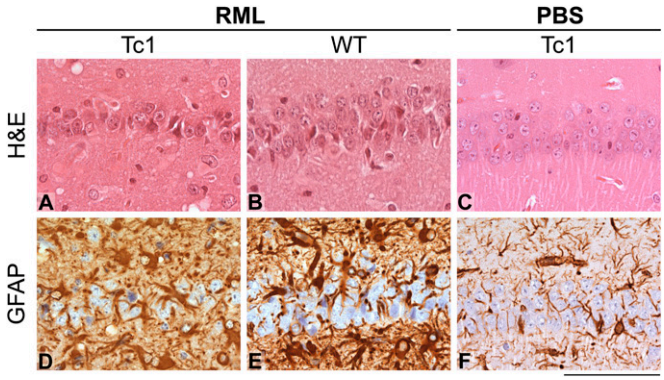

Fig. S5. Neuropathological features of Chandler/RML prion transmission to Tc1 mice. Panels show a high-power view of the hippocampus. (Scale bar, 80 μm.) *A–C* are stained with hematoxylin and eosin (H&E) to show neuronal loss. The hippocampal neuronal ribbon is thinner (2–3 cells thick) in Tc1 mice (*A*) compared with wild-type litter mate controls (5–6 cells thick) (*B*). PBS inoculated Tc1 mice (*C*) have a healthy neuronal ribbon, indicating that the differential neuronal loss is the result of increased susceptibility to neuronal death following prion infection. Gliosis is shown by staining with an anti-glial fibrillary acid protein (anti-GFAP) antibody (*D–F*). Both Tc1 mice (*D*) and wild type (*E*) show strongly reactive astrocytes following prion infection compared with PBS-inoculated mice (*F*) and for Tc1 mice, this staining is seen in the neuronal ribbon, indicating neuronal loss replaced by reactive astrocytes.

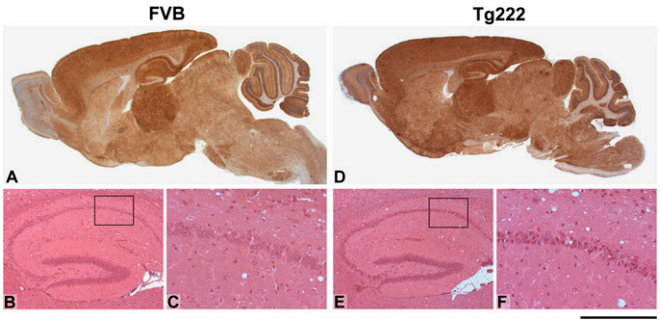

Fig. S6. Histological features of Chandler/RML prion transmission to Tg222 mice. Comparison is shown between FVB/NHsd controls (*A*–*C*) and Tg222 mice (*D*–*F*). PrP^{Sc} distribution is visualized by staining with the anti-PrP monoclonal antibody ICSM35. Mild neuronal loss in the CA1 region of the hippocampus is shown by hematoxylin and eosin (H&E) staining (*B* and *C* and *E* and *F*). Overall, the pattern of PrP^{Sc} distribution, and the degree of neuronal loss in hippocampus, show no difference between both groups. (Scale bar, 3 mm in *A* and *D*, 640 μm in *B* and *E*, and 160 μm in *C* and *F*.)

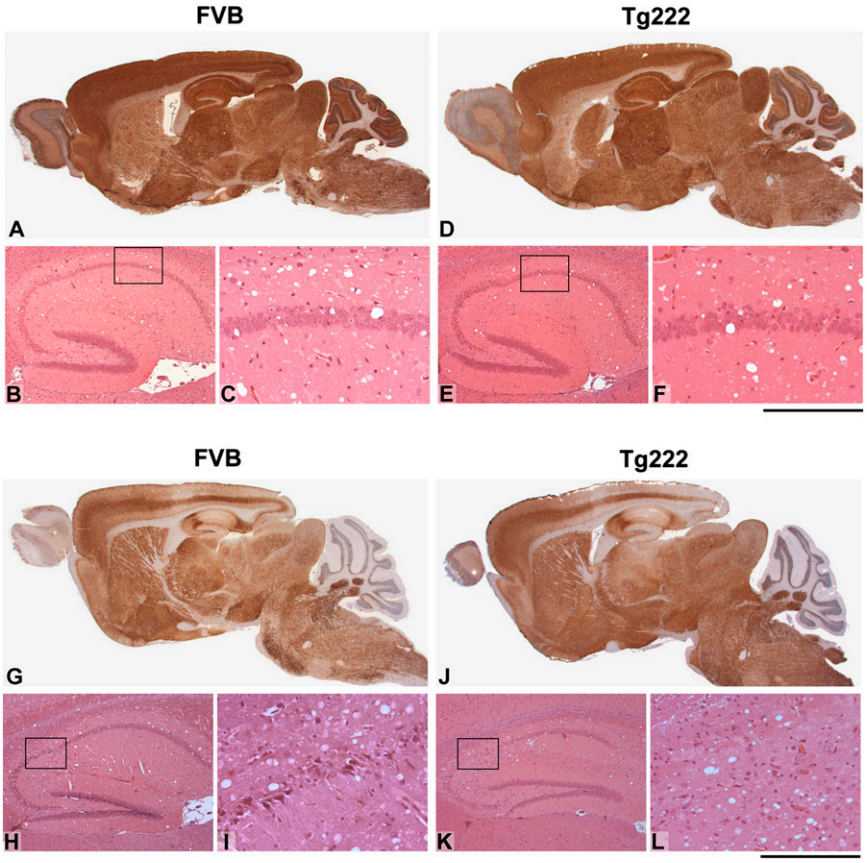

Fig. S7. Histological features of ME7 and MRC2 prion transmission to Tg222 mice. *A*–*F* show ME7 transmission and *G*–*L* show MRC2 transmission. Comparison is shown between FVB/NHsd controls (*A*–*C*) and Tg222 mice (*D*–*F*). PrP^{Sc} distribution is visualized by staining with the anti-PrP monoclonal antibody ICSM35. Spongiosis and neuronal loss were visualized by hematoxylin and eosin (H&E) staining (*B* and *C* and *E* and *F*). No neuronal loss and mild-to-moderate spongiosis was observed in the hippocampus for both groups. Overall, the pattern of PrP^{Sc} distribution and spongiosis show no difference between both groups. (Scale bar, 3 mm in *A* and *D*, 640 μm in *B* and *E*, and 160 μm in *C* and *F*.) Comparison is shown between FVB/NHsd controls (*G*–*I*) and Tg222 mice (*J*–*L*). PrP^{Sc} distribution is visualized by staining with the anti-PrP monoclonal antibody ICSM35. Spongiosis and neuronal loss were visualized by H&E staining (*H* and *I* and *K* and *L*). Overall, the pattern of PrP^{Sc} distribution shows no difference between both groups. There is mild neuronal loss in the CA2 region of the hippocampus in FVB mice (*H* and *I*); however, the neuronal loss is more severe in some Tg222 animals (*K* and *L*). This loss was not seen in all Tg222 animals and is not statistically significant when the whole group is considered. (Scale bar, 3 mm in *G* and *J*, 640 μm in *H* and *K*, and 160 μm in *I* and *L*.)

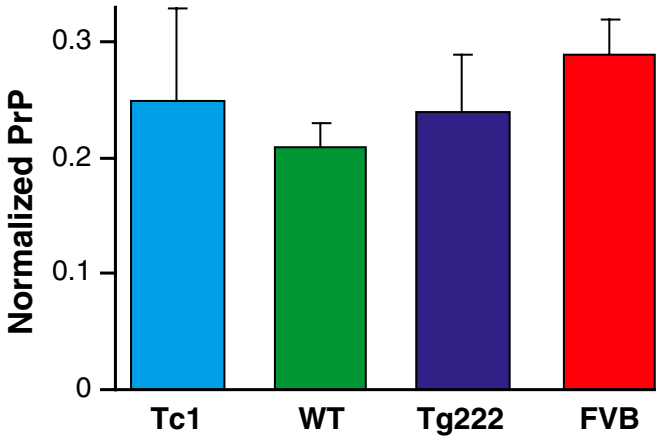

Fig. S8. PrP^c levels in Tc1, Tg222, and wild-type mice. PrP^c levels (μg/mL) were determined in triplicate using 10% (wt/vol) brain homogenate for Tc1 and WT control ($n = 3$) and both Tg222 and FVB ($n = 3$) in a PrP-specific ELISA. Data are shown normalized by total protein content (μg/mL and ×1,000) as determined by a BCA assay (mean ± SD). No significant difference was seen between Tc1 and controls or between Tg222 and wild-type animals.

Table S1. Top 30 genes ranked by R^2 value

Probe ID	Symbol	*P* value	R^2	Fold difference
1460674_at	*Paqr7*	0.0008	0.992	1.28
1437687_x_at	*Fkbp9*	0.0021	0.992	0.84
1424289_at	*Osgin2*	0.0077	0.969	0.67
1419601_at	*Kcnj10*	0.0008	0.963	1.34
1417571_at	*Mpg*	0.0012	0.950	3.23
1428230_at	*Prkcn*	0.0008	0.949	0.06
1434738_at	*Tm2d3*	0.0056	0.935	0.61
1416446_at	*Tmem30a*	0.0056	0.935	0.86
1435392_at	*Wdr17*	0.0047	0.933	0.61
1428100_at	*Sfrs1*	0.0024	0.927	0.68
1427958_at	*Abhd10*	0.0020	0.926	0.45
1436266_x_at	*Cbx1*	0.0003	0.924	1.81
1421756_a_at	*Gpr19*	0.0078	0.922	1.28
1428309_s_at	*Pdrg1*	0.0009	0.922	0.52
1427689_a_at	*Tnip1*	0.0034	0.917	1.47
1426167_a_at	*Camk4*	0.0018	0.915	6.21
1424568_at	*Tspan2*	0.0066	0.908	0.84
1448374_at	*Med28*	0.0025	0.903	5.0
1428645_at	*Gnai3*	0.0005	0.903	0.71
1455732_at	*2610510E02Rik*	0.0021	0.902	0.79
1435788_at	*AK013823*	1.8E-06	0.901	0.40
1438089_a_at	*Bclaf1*	0.0014	0.898	0.68
1435719_at	*Orc3l*	0.0034	0.889	0.15
1453172_at	*Hsa13*	1.5E-05	0.886	4.96
1424222_s_at	*Rad23b*	0.0018	0.871	0.74
1450437_a_at	*Ncam1*	0.0006	0.870	1.21
1437031_at	*Acsl6*	0.0020	0.870	0.57
1417648_s_at	*Snx5*	0.0005	0.865	0.65
1454424_at	*2610040L17Rik*	0.0016	0.859	0.23
1437236_a_at	*Zfp110*	0.0018	0.854	0.36

P value is calculated by Limma and expresses the difference in expression level between NZW and (shortest incubation time) and C57BL/6 (longest incubation time) with a false discovery rate of 0.01 (ref. 1). R^2 value measures the correlation in expression time with incubation time across all five mouse strains. Fold difference is the expression level of NZW relative to C57BL/6.

1. Smyth GK (2004) Linear models and empirical Bayes methods for assessing differential expression in microarray experiments. *Stat Appl Genet Mol Biol* 3: Article 3.